JOURNAL OF SOLID STATE CHEMISTRY 68, 300–306 (1987)

Electrical Resistivity of Pyrochlore Compounds $R_2Mo_2O_7$ (R = Nd, Sm, Gd, Tb, Y)

J. E. GREEDAN,* M. SATO,† NAUSHAD ALI,‡ AND W. R. DATARS‡

*Institute for Materials Research and Departments of *Chemistry and ‡Physics, McMaster University, Hamilton, Ontario, Canada L8S 4M1*

Received July 1, 1986; in revised form September 23, 1986

The electrical resistivity of $R_2Mo_2O_7$ (R = Nd, Sm, Gd, Tb, Y) pyrochlores was measured in the temperature range 4.2 to 300 K. Metallic behavior is observed for $Nd_2Mo_2O_7$, $Sm_2Mo_2O_7$, and $Gd_2Mo_2O_7$ which have relatively high magnetic ordering temperatures due to ferromagnetism on the molybdenum sublattice. A clear drop in resistivity is observed near the magnetic ordering point for all metallic materials. A resistance minimum observed at low temperatures, which may be due to the magnetic ordering of the rare-earth sublattice, is not completely understood. $Tb_2Mo_2O_7$ and $Y_2Mo_2O_7$, which show no molybdenum sublattice ordering down to 4.2 K, are semiconductors. However, the temperature dependence of the resistivity is not exponential. This unusual resistivity behavior is typical of degenerate semiconductors.

Introduction

Recently, Subramanian and colleagues have investigated the magnetic and electrical properties of $R_2Mo_2O_7$ (R = Sm–Yb, Y) pyrochlores (*1, 2*). They reported semiconducting behavior with low resistivity and a low activation energy for R = Gd–Yb, Y, and semimetallic or metallic conduction for $Sm_2Mo_2O_7$. All compounds were reported to exhibit magnetic ordering in the neighborhood of 77 K. Their experimental results were, however, only obtained above 77 K and there have been no other studies of the physical properties of these compounds.

In a previous study (*3*), we found a large change in the magnetic properties of the $R_2Mo_2O_7$ series between $Gd_2Mo_2O_7$ and $Tb_2Mo_2O_7$. The materials R = Nd, Sm, and Gd show evidence for long-range magnetic order of the ferro- or ferrimagnetic type at relatively high temperatures (80–95 K) arising from ferromagnetic interactions on the Mo sublattice. On the other hand, those phases for R = Tb–Yb, Y do not order in the long-range sense down to 4.2 K. $Y_2Mo_2O_7$ and solid solutions $(La_xY_{1-x})_2Mo_2O_7$ appear to be spin glasses or cluster glasses with competing ferromagnetic and antiferromagnetic exchange interactions (*4, 5*). To determine whether the magnetic and electrical properties are correlated, we undertook resistivity measurements for selected members of the $R_2Mo_2O_7$ series (R = Nd, Sm, Gd, Tb, Y and the solid solution $La_{0.3}Y_{0.7}$) in the temperature range 2.4–300 K.

Experimental

Samples of $R_2Mo_2O_7$ were prepared by heating an appropriate molar ratio mixture

† Permanent address: Kochi Technical College, Monobe Otsu 200-1, Nangoku-Shi, Kochi-Ken 783, Japan.

0022-4596/87 $3.00

of MoO_2 and R_2O_3 (or Tb_4O_7) in a CO/CO_2 buffer gas at 1400°C. Details of the preparation and characterization of these compounds are given elsewhere (*3*).

Although an attempt was made to grow a single crystal from the melt with a modified tri-arc furnace on a molybdenum hearth, the effort was not successful. Thus, the electrical resistivity measurements were done with sintered materials with dimensions of approximately 2 × 2 × 10 mm. The data were obtained by a conventional four-probe method in the temperature range 4.2 to 300 K. Electrical contacts were made with silver paste between four beryllium–copper springs with the sample mounted on an integrated circuit holder. Temperature was monitored with a calibrated carbon–glass thermometer mounted near the sample.

Results and Discussion

Table I summarizes the magnetic data obtained in a previous study (*3*). The critical temperature, T_c, corresponds to the ferromagnetic ordering of the molybdenum sublattice. The second temperature, T_2, is attributed to the onset of induced order in the rare-earth sublattice through coupling to the transition metal sublattice as in $Yb_2V_2O_7$ and $Tm_2V_2O_7$ (*6*). These temperatures were obtained from data taken in a nearly zero applied field. The T_c's are well-defined, as are the T_2's for R = Nd and Sm, whereas the second transition for R = Gd occurs over a broader temperature range.

TABLE I

MAGNETIC DATA FOR $R_2Mo_2O_7$

	T_c[a] (K)	T_2 (K)
$Nd_2Mo_2O_7$	97	20–25
$Sm_2Mo_2O_7$	93	20–25
$Gd_2Mo_2O_7$	83	30–50

[a] Data taken from σ^3 (0.0045 T) vs T plot where σ is the magnetic moment.

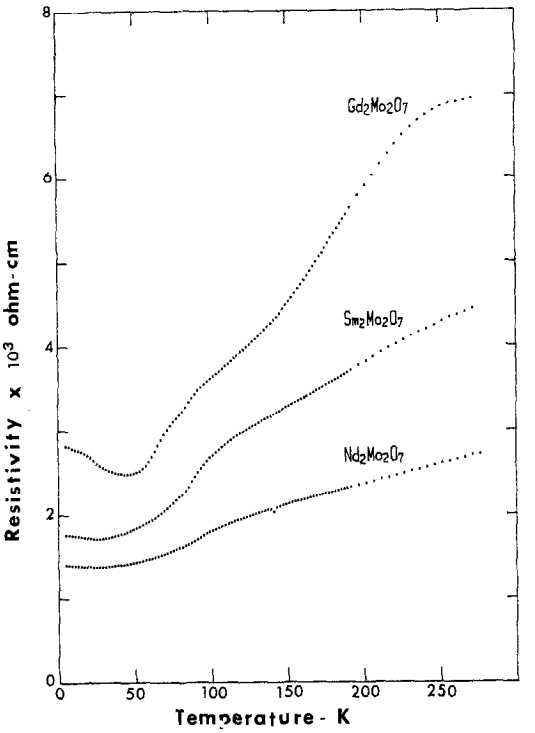

FIG. 1. Electrical resistivity versus temperature for $Gd_2Mo_2O_7$, $Sm_2Mo_2O_7$, and $Nd_2Mo_2O_7$.

Temperature dependences of the resistivity are given in Fig. 1 for $Nd_2Mo_2O_7$, $Sm_2Mo_2O_7$, and $Gd_2Mo_2O_7$, and in Fig. 2 for $Tb_2Mo_2O_7$ and $Y_2Mo_2O_7$. Clearly, these two groups of compounds show very different behavior. For R = Nd → Gd, the resistivity has a temperature dependence normally associated with metals or semimetals while R = Tb and Y are semiconducting. Although in the case of the former group the magnitudes of the resistivities are in the 10^{-3} ohm-cm range, considerably higher than in normal metals, there are some relevant points to consider. First, these samples consist of sintered, polycrystalline disks, not single crystals, and thus the measured resistivities include effects of intergranular resistances. Second, the *d* elec-

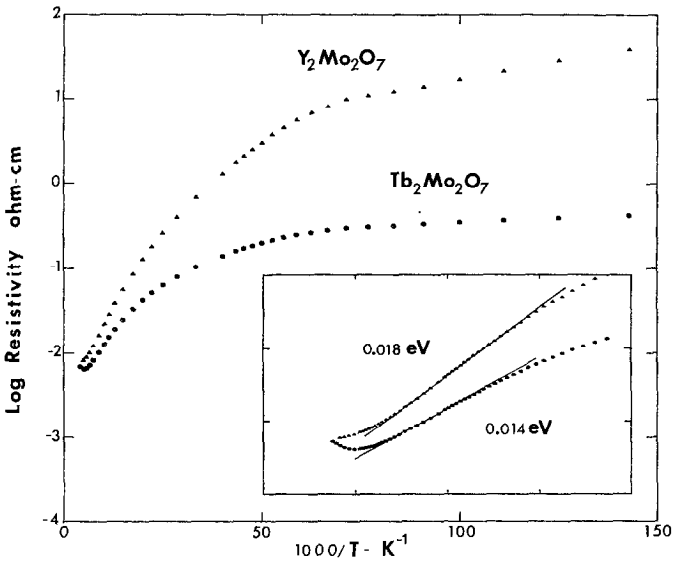

FIG. 2. Electrical resistivity versus temperature for $Tb_2Mo_2O_7$ and $Y_2Mo_2O_7$. The inset showed data for the temperature range 200 K to 67 K (1000/T = 5.0 to 15.0).

trons in these compounds must be highly correlated, as evidenced by the appearance of spontaneous magnetism at low temperatures. Similar materials, i.e., highly correlated, metallic transition metal oxides such as V_2O_3 (*12*), have resistivities in this same 10^{-3} ohm-cm range. Clearly, a more detailed study of the transport properties coupled with information on electronic structure will be necessary to understand the relatively high, yet metallike resistivity in these complex materials.

Our results differ from those obtained by Subramanian *et al.* (*1*), who observed the transition from metallic to semiconducting behavior between $Sm_2Mo_2O_7$ and $Gd_2Mo_2O_7$. Further, our value for the 300 K resistivity of $Sm_2Mo_2O_7$ ($\sim 4.7 \times 10^{-3}$ Ω cm) is similar to that reported previously, but we observe a strong temperature dependence below 300 K whereas Subramanian *et al.* found a nearly temperature independent resistivity. A very recent report of thermopower data on, presumably, the same samples of Ref. (*1*) argues for an activated transport process for R = Yb to Gd (*7*). This is consistent with our results except for Gd where the resistivity data presented here differ markedly from those of Ref. (*1*).

Turning to a closer examination of Fig. 1, all three metallic compounds exhibit two common features: (i) a sharp change in the slope of ρ vs T near 100 K and (ii) a minimum in ρ vs T at lower temperatures. The first feature is widely observed in metallic materials containing localized or highly correlated *f* or *d* electrons which have a transition to a magnetically ordered state. In general, the total resistivity is the sum of three leading contributions

$$\rho(T) = \rho_0 + \rho_{ph}(T) + \rho_s(T)$$

where ρ_0 is the residual resistivity due to scattering of conduction electrons by impurities and is temperature independent, ρ_{ph} is due to phonon scattering, and ρ_s is due to scattering by the spins of the localized or highly correlated electrons (*8*). At temperatures greater than T_c, i.e., where the spins are disordered, ρ_s is usually temperature independent and $\rho(T)$ is dominated by the phonon term. Below T_c, ρ_s decreases with decreasing temperature as the spins begin to order on the magnetic sublattice and $\rho(T)$

decreases more rapidly than expected from the phonon term alone (*8*). Also, near T_c, a logarithmic divergence in $d\rho/dT$ versus T is usually seen (*9*). This is observed in our data as shown in Fig. 3. Here the solid line is given by $d\rho/dT = A \log|\varepsilon| + B$ where $\varepsilon = ((T - T_c)/T_c)$. The T_c's extracted from this analysis are 94 K for $Nd_2Mo_2O_7$, 86 K for $Sm_2Mo_2O_7$, and 83 K for $Gd_2Mo_2O_7$ and in fair agreement with values obtained from the magnetization measurements. At present, the appearance of a second peak in $d\rho/dT$ for $Gd_2Mo_2O_7$ at about 62 K is not understood but may indicate a further magnetic spin reorientation. Thus, the first feature in ρ vs T for the metallic $R_2Mo_2O_7$ compounds is associated with the long-range magnetic order of the Mo^{4+} sublattice.

The origin of the second feature, the resistivity minimum, is more difficult to understand. Circumstantial evidence suggests that this effect may also be associated with the magnetic properties. Note that the positions of the resistivity minima, about 25, 25, and 40 K for R = Nd, Sm, and Gd respectively, correlate reasonably well with the T_2 values, the temperature ranges over which the rare-earth sublattice begins to exhibit some kind of induced order. At present, information regarding the nature of the magnetic structure in this temperature range is not available. Neutron diffraction experiments on $Nd_2Mo_2O_7$ are planned.

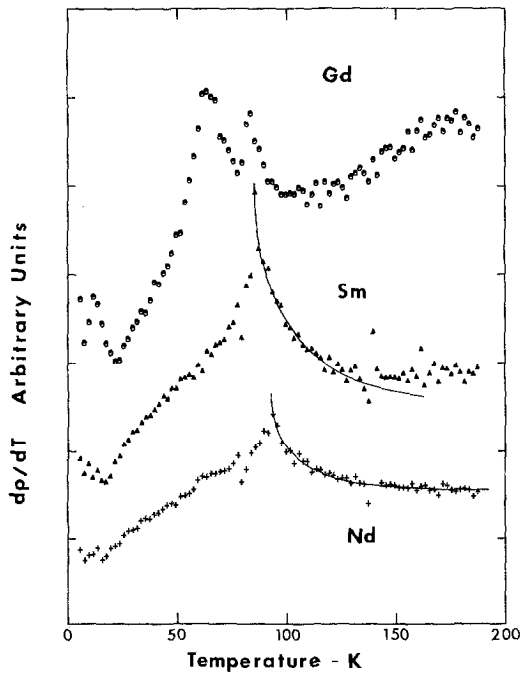

FIG. 3. $d\rho/dT$ versus T for $Gd_2Mo_2O_7$ (Gd), $Sm_2Mo_2O_7$ (Sm), and $Nd_2Mo_2O_7$ (Nd). The solid lines are fits to the function $d\rho/dT = A \log((T - T_c)/T_c) + B$.

Returning to the data of Fig. 1, one notices that the magnitude of the resistivity at all temperatures increases systematically from Nd to Sm to Gd. Note also that the temperature dependence of the resistivity above T_c for $Gd_2Mo_2O_7$ is different from that for $Nd_2Mo_2O_7$ and $Sm_2Mo_2O_7$. For the latter two materials, ρ vs T is nearly linear from T_c to 300 K. Such behavior is usually ascribed to phonon scattering. For $Gd_2Mo_2O_7$ a T^2 dependence is observed in the region from 90 to 150 K, as shown in Fig. 4, followed by an approach to saturation near 300 K. The solid line in Fig. 4 is a least-squares fit to the function $\rho = \rho_0 + \alpha T^2$, where α is 6.9×10^{-8} ohm-cm K^{-2}. This value of the T^2 coefficient is about 10^3 times that for most transition metal and metallic oxide materials such as Pt or RuO_2 (*10, 11*), but is of the same order as found for highly correlated systems such as Mn (*10*), V_2O_3 (*12*), or CrO_2 (*13*). The relatively high temperatures for which the T^2 dependence is observed is unusual but CrO_2 also shows such behavior in a similar range. The appearance of a T^2 term in the resistivity for a material above its magnetic T_c is attributed to electron–electron scattering as first proposed by Baber (*14*). Considering the magnitude of this term for $Gd_2Mo_2O_7$ it is reasonable to conclude that a very high degree of correlation exists in this material and that the degree of correlation increases systematically from Nd to Gd in the $R_2Mo_2O_7$ series. For a recent discussion of the role of electron correlation in enhancing the mag-

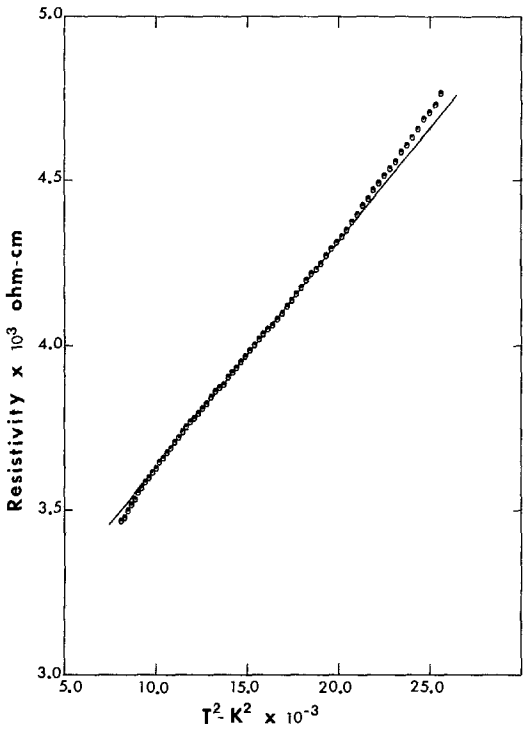

FIG. 4. The T^2 dependence of the resistivity for $Gd_2Mo_2O_7$ in the range 90 to 150 K.

nitude of the T^2 term see Moriya (*15*) and references therein.

As already noted, for R = Tb the electrical properties change completely to exhibit semiconducting behavior. Semiconducting behavior is also noted for $Y_2Mo_2O_7$. An examination of Fig. 2 shows that the usual, linear log ρ vs T^{-1} dependence is not found for either material over the entire temperature range covered in these measurements. Our results are in fair agreement with those of Subramanian *et al.* in the temperature range where the two studies overlap. These authors report an activated conductivity for both $Tb_2Mo_2O_7$ and $Y_2Mo_2O_7$ with activation energies of 7.0×10^{-3} and 1.3×10^{-2} eV, respectively, which can be compared to our results of 1.4×10^{-2} and 1.8×10^{-2} eV, respectively, from data in the range 200 to 70 K (see inset Fig. 2). The present study extends to much lower temperatures and, as can be seen from Fig. 2, the resistivities for both materials approach a saturation value. This type of behavior has been observed in highly doped metal oxide semiconductors, such as $Li_xNi_{1-x}O$ (*16*), and in semimetallic alloys, such as Bi–Sb (*17*). Several models exist to explain data of this type including polaron formation or impurity band formation but, lacking detailed transport data, further speculation here is unwarranted. The basic conclusion that can be drawn is that the semiconducting members of this series appear to behave as highly doped, nearly degenerate semiconductors.

The observation of metallic or semiconducting behavior as a function of R in the $R_2Mo_2O_7$ series is unique for this broad class of pyrochlore metal oxides. All known pyrochlores of the type where R is a rare-earth and M is a 3*d*, 4*d*, or 5*d* transition element are semiconductors (*1, 18–21*). A qualitative explanation has been advanced previously (*20*). This model invokes two competing interactions, the first involving t_{2g} orbitals on M and $p\pi$ orbitals on the 48*f* O atoms—an M–Oπ interaction—and the second involving $p\sigma$ orbitals on R and the same set of O atoms. This results in a set of partially occupied M–O π^* levels which lie just below an empty R–O σ^* band. If the R–O σ interaction is sufficiently strong the M–O π^* levels may be localized or at least form highly correlated Hubbard bands. Now the strength of the R–O σ interaction is expected to decrease with increasing basicity or increasing size of the R atom, i.e., in the order Lu → La across the rare-earth series. All of the electrical transport data presented here and in previous studies for the $R_2Mo_2O_7$ series are consistent with this relatively simple idea. All compounds from R = Yb to Tb are semiconductors with quasi-localized $4d^2$ electrons; R = Gd is a highly correlated metal or semimetal and R = Sm and Nd show more normal behavior consistent with a broader Mo–O π^* band.

In the context of the above, it is interesting to examine the electrical properties of the solid solution $(La_{0.3}Y_{0.7})_2Mo_2Y_7$. For this composition, the average radius of the atom in the large cation site is essentially equal to that of Gd, one of the metallic members of the series. From the results plotted in Fig. 5, it is evident that not only are metallic properties not observed but the resistivity of this material is also much higher at all temperatures than any of the other $R_2Mo_2O_7$ pyrochlores studied. In fact, the electrical behavior of $(La_{0.3}Y_{0.7})_2Mo_2O_7$ is quite complex, showing three distinct linear regions in the log ρ vs T^{-1} plot with activation energies as follows: 300–130 K, 0.067 eV; 130–40 K, 0.046 eV; and 40 to 26 K, 0.035 eV. This shows that it is naïve to expect the $(R,R')_2Mo_2O_7$ solid solutions to behave as the corresponding well-ordered $R_2Mo_2O_7$ phases. The same observation was made in a study of the magnetic properties of the La_xY_{1-x} solid solutions where all of these materials exhibit spin–glass-like behavior, even the compositions $La_{0.3}Y_{0.7}$, $La_{0.4}Y_{0.6}$, and $La_{0.55}Y_{0.45}$ which have the same lattice constants as the ferromagnetic Gd, Sm, and Nd compounds (*3, 5*). Apparently, the disorder on the rare-earth site is a sufficient perturbation on the Mo–O π^* subsystem to induce localization, probably through a mechanism such as that suggested by Anderson (*22*).

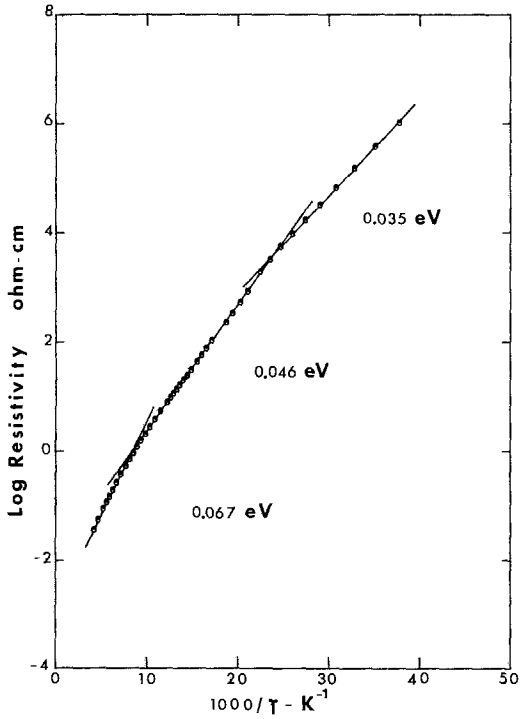

FIG. 5. Electrical resistivity versus temperature for $(La_{0.3}Y_{0.7})_2Mo_2O_7$.

At this point, it is worth noting again the correlation between magnetic and electrical properties. Among the known $R_2Mo_2O_7$ compounds all of the metallic phases are ferromagnetic and the semiconducting phases show spin–glass-like or cluster–glass behavior. We have pointed out previously that in pyrochlore-structure materials with only short-range, nearest neighbor antiferromagnetic interactions, that spin–glass-like properties can be expected (*4*). In metallic systems long-range coupling via the conduction electrons can exist, giving rise to three-dimensional ferromagnetic order.

Finally, the properties of the $R_2Mo_2O_7$ pyrochlore series can be compared with those of the $RTiO_3$ perovskites, which have been the subject of recent, intensive investigation in our laboratory (*23*). In both series the high-temperature electrical and magnetic properties are determined by the transition metal–oxygen sublattices which are topologically similar, consisting of three-dimensional networks of corner-shared MO_6 octahedra. The R^{3+} ions interact with the M–O network in two ways. In the $RTiO_3$ series the Ti–O–Ti bridging angle between two octahedra varies with the size of R from 155° (R = La) to 140° (R = Y). For the $R_2Mo_2O_7$ phases, the detailed structures are not known but the Mo–O–Mo angle should lie near 130°. Little change in this angle with R is anticipated. In both cases, there will be an "inductive" effect, as discussed earlier, where R^{3+} competes

with the transition metal ion and withdraws electron density from the M–O π bonding network. The magnitude of the inductive effect increases as the size of the R^{3+} ion decreases. There occurs in both series a metal to semiconductor transition as R^{3+} decreases in size. For the $RTiO_3$ compounds the metal/semiconductor boundary is between Ce and Pr while for the $R_2Mo_2O_7$ group it is found between Gd and Tb. For the pyrochlores the metal–semiconductor transition is due purely to the inductive effect while for the perovskites it is difficult to separate this from the geometric effect. It is also worth noting that similar behavior has been seen in pyrochlores based on Ru^{4+} (*22, 23*). Here the phase $Bi_2Ru_2O_7$ is metallic while those pyrochlores with a rare earth on the large cation site are semiconducting. It has been argued that the Bi 6*s* levels are involved in the conduction band of $Bi_2Ru_2O_7$.

There also exists a continuous transition between ferromagnetic and antiferromagnetic net magnetic exchange as a function of R in the two series. In the perovskite series the members with large R^{3+} show antiferromagnetic behavior on the Ti–O sublattice, R = La, Ce, and Pr, while ferromagnetism appears for small R^{3+}, R = Gd → Yb. The reverse is true for the molybdenum pyrochlores with ferromagnetism for R = Nd → Gd and predominantly antiferromagnetic interactions for R = Tb → Y. These differences may be due in part to the electronic configurations of the two transition metal ions involved. Ti^{3+}, $3d^1$, and Mo^{4+}, $4d^2$, but a detailed explanation is not presently available.

Acknowledgment

This work was supported by the Natural Science and Engineering Research Council of Canada.

References

1. M. S. Subramanian, G. Aravamudan, and G. V. Subba Rao, *Mater. Res. Bull.* **15,** 1401 (1980).
2. R. Ranganathan, G. Rangarajan, R. Srivivasan, M. A. Subramanian, and G. V. Subba Rao, *J. Low Temp. Phys.* **52,** 481 (1983).
3. M. Sato, Xu Yan, and J. E. Greedan, *Z. Anorg. Alleg. Chem.*, **540/541,** 177 (1986).
4. J. E. Greedman, M. Sato, Xu Yan, and F. Razavi, *Solid State Commun.* **59,** 895 (1986).
5. M. Sato and J. E. Greedan, *J. Solid State Chem.* **67,** 248–253 (1987).
6. L. Soderholm, C. V. Stager, and J. E. Greedan, *J. Solid State Chem.* **43,** 175 (1982).
7. V. V. Rao, G. Rangarajan, and R. Srinivasan, *J. Phys. Chem. Solids* **47,** 395 (1986).
8. A. J. Dekker, *J. Appl. Phys.* **36,** 906 (1965); P. G. deGennes and J. Friedel, *J. Phys. Chem. Solids* **4,** 71 (1958).
9. P. P. Craig, W. I. Goldburg, T. A. Kitchens, and J. I. Budnick, *Phys. Rev. Lett.* **19,** 1334 (1967).
10. G. K. White and S. B. Woods, *Philos. Trans. R. Soc. London* **251,** 273 (1959).
11. W. D. Ryden, A. W. Lawson, and C. C. Sartain, *Phys. Rev. B* **1,** 1494 (1970).
12. D. B. McWhan and T. M. Rice, *Phys. Rev. Lett.* **22,** 887 (1969).
13. D. S. Rodbell, J. M. Lommel, and R. C. De Vries, *J. Phys. Soc. Japan* **21,** 2430 (1966).
14. W. G. Baber, *Proc. R. Soc. (London) A* **158,** 383 (1937).
15. T. Moriya, *J. Magn. Magn. Mater.* **14,** 1 (1979).
16. A. J. Spring-Thorpe, I. G. Austin, and B. A. Austin, *Solid State Commun.* **3,** 143 (1965).
17. A. L. Jain, *Phys. Rev.* **114,** 1521 (1959).
18. G. V. Bazuev, O. V. Makarova, V. Z. Oboldin, and G. P. Shveibin, *Dokl. Akad. Nauk SSSR* **230,** 869 (1976); T. Shin-ike, G. Adachi, and J. Shiokawa, *Mater. Res. Bull.* **12,** 1149 (1977).
19. H. Fujinaka, N. Kinomura, M. Koizumi, Y. Mizamoto, and S. Kume, *Mater. Res. Bull.* **14,** 1133 (1979).
20. A. W. Sleight and R. J. Bouchard, *NBS Spec. Publ. 364,* "Solid State Chemistry," Proceedings of 5th Materials Research Symposium, July 1972.
21. R. J. Bouchard and J. L. Gillson, *Mater. Res. Bull.* **6,** 669 (1971); C.N.R. Rao and G. V. Subba Rao, *Phys. Status Solidi A* **1,** 597 (1970).
22. P. W. Anderson, *Phys. Rev.* **109,** 1492 (1958).
23. J. E. Greedan, *J. Less Common Met.* **111,** 335 (1985) and references therein.
24. P. A. Cox, R. G. Egdell, J. B. Goodenough, A. Hamnett, and C. C. Naish, *J. Phys. C: Solid State Phys.* **16,** 6221 (1983).
25. P. A. Cox, J. B. Goodenough, P. J. Tavener, D. Telles, and R. G. Edgell, *J. Solid State Chem.* **62,** 360 (1986).